ČESKÉ VYSOKÉ UČENÍ TECHNICKÉ V PRAZE
FAKULTA STROJNÍ

DEPARTMENT OF ENVIRONMENTAL ENGINEERING

UNIVERSITY CENTRE FOR ENERGY EFFICIENT BUILDINGS UCEEB

TITLE

TRNSYS TYPE 223 V0.1

MODEL OF GLAZED LIQUID PHOTOVOLTAIC-THERMAL SOLAR COLLECTOR BASED ON DETAILED CONSTRUCTION PARAMETERS AND ENERGY BALANCE

AUTHORS

Nikola Pokorny (UCEEB CVUT)

Tomas Matuska (UCEEB CVUT, FME CVUT)

PAGES 20

ANNEXES -

DATE November 2015

CZECH TECHNICAL UNIVERSITY IN PRAGUE | FACULTY OF MECHANICAL ENGINEERING

DEPARTMENT OF ENVIRONMENTAL ENGINEERING

UNIVERSITY CENTRE FOR ENERGY EFFICIENT BUILDINGS UCEEB

CONTENTS

1. INTRODUCTION

In order to optimize the design of the glazed photovoltaic-thermal (PV-T) collector, a detailed mathematical model has been developed and implemented into the TRNSYS environment. Reason for implementation in the TRNSYS was to have a model, which includes the sufficient amount of collector design parameters for the optimization process. Current model of glazed PV-T collector in TRNSYS type 50b [1] does not consider a detailed construction of the collector and change of important collector parameters during the different climate and operational conditions (collector heat loss coefficient, fin efficiency factor, etc.). Currently, several steady state models [2,3,4] and dynamic models of PV-T collector [5,6] exist. These models are suitable for determination of thermal characteristics of PV-T collector, but they have not been implemented into TRNSYS type to be used in system simulations.

Advantage of implemented model is that model calculates energy flow from PV-T absorber surface to ambient and energy flow from PV-T absorber surface to liquid, all in every time step. The detailed model of glazed PV-T collector allows to define a number of design and physical parameters of collector configuration: geometry, electric properties of PV cells, thermo-physical properties of materials used PV-T collector, etc. Inputs of the model are conventional: weather and operation conditions. Main outputs of the model are useable thermal and electric power, absorber temperature and outlet liquid temperature.

Mathematical model has been developed with use of Florschuetz approach [7]. The model uses detailed energy flows balance of PV-T collector, expanded for photovoltaic conversion. Calculation procedure of the model solves the external and internal energy balance of the PV-T absorber. Both balances proceeds in the iteration loop.

2. SUMMARY

2.1. Input list

Nr.	Symbol	Name	Unit	Range
1	G	Incident irradiance	W/m^2	[0;+inf]
2	t_a	Ambient temperature	°C	[-inf;+inf]
3	w	Wind velocity	m/s	[0;+inf]
4	$\dot{m}$	Mass flow rate	kg/h	[0;+inf]
5	t_{in}	Inlet fluid temperature	°C	[-inf;+inf]
6	θ	Incidence angle	degrees	[0;+inf]

2.2. Parameter list

Nr.	Symbol	Name	Unit	Range
1	β	Slope angle	°	[0;+inf]
2	ε_z	Adjacent frontal surface emissivity	-	[0;1]
3	p	Gas pressure between glazing and PV-T absorber	kPa	[0;+inf]
4	H_g	Gross height	m	[0;+inf]
5	L_g	Gross length	m	[0;+inf]
6	H_a	Aperture height	m	[0;+inf]
7	L_a	Aperture length	m	[0;+inf]
8	d_p	Gap size between glazing and PV-T absorber	m	[0;+inf]
9	d_z	Gap size between PV-T absorber and Frame	m	[0;+inf]
10	λ_{abs}	Thermal conductivity of the PV-T absorber	W/m.K	[0;+inf]
11	d_{abs}	Thickness of absorber	m	[0;+inf]
12	α	Normal solar absorptance	-	[0;1]
13	ε_{abs_p}	Front surface emissivity of PV-T absorber	-	[0;1]

14	ε_{abs_z}	Back surface emissivity of PV-T absorber	-	[0;1]
15	L	Length of riser pipes	m	[0;+inf]
16	n	Number of riser pipes	-	[0;+inf]
17	W	Distance between the riser pipes	m	[0;+inf]
18	D_i	Riser pipe internal diameter	m	[0;+inf]
19	a	Average bond width	m	[0;+inf]
20	b	Average bond thickness	m	[0;+inf]
21	λ_{abs}	Thermal conductivity of bond	W/m.K	[0;+inf]
22	ξ	Mixing ratio of propylene glycol in water	-	[0;1]
23	d_{p12}	Thickness of cover glazing	m	[0;+inf]
24	λ_{p12}	Thermal conductivity of cover glazing	W/m.K	[0;+inf]
25	τ	Normal solar transmittance	-	[0;1]
26	ε_{p1}	External surface emissivity of cover glazing	-	[0;1]
27	ε_{p2}	Internal surface emissivity of cover glazing	-	[0;1]
28	d_{z12}	Thickness of back side insulation	m	[0;+inf]
29	λ_{z12}	Thermal conductivity of back side insulation	W/m.K	[0;+inf]
30	ε_{z1}	External frame surface emissivity	-	[0;1]
31	ε_{z2}	Internal frame surface emissivity	-	[0;1]
32	d_{b12}	Thickness of insulation (edge side)	m	[0;+inf]
33	λ_{b12}	Thermal conductivity of insulation (edge side)	W/m.K	[0;+inf]
34	η_{ref}	Reference electrical efficiency of PV cells	-	[0;1]
35	γ_{ref}	Temperature coefficient of PV cell efficiency	-	[0;1]
36	T_{ref}	Temperature for cell reference efficiency	°C	[-inf;+inf]
37	b_0	1-st order IAM	-	[0;0.2]
38	*gas_layer*	Gas filling	-	[0;1]

39	n_{col}	Number of collectors	-	[1;+inf]
40	r	Packing factor for PV cells	-	[0;1]

2.3. Output list

Nr.	Symbol	Name	Unit	Range
1.	$\dot{m}$	Outlet mass flow rate	kg/h	[0;+inf]
2.	Q_t	Thermal power	W	[-inf;+inf]
3.	Q_e	Electrical power	W	[-inf;+inf]
4.	T_{out}	Outlet fluid temperature	°C	[-inf;+inf]
5.	T_{abs}	Mean absorber temperature	°C	[-inf;+inf]

3. MATHEMATICAL REFERENCE

The model uses energy balance of PV-T collector, expanded for photovoltaic conversion. Calculation procedure of the model solves the external and internal energy balance of the PV-T absorber. Both balances proceeds in the iteration loop. The mathematical model solves energy balance under steady state conditions, thermal capacity of the PV-T collector is not considered. Procedure of the calculation is described by Matuska [8] includes correlation for heat transfer coefficient.

3.1. External energy balance of the PV-T absorber

The core of the external energy balance of the PV-T absorber is an iteration loop for calculation of temperature distribution for main surfaces (temperature levels) of solar collector, see in Fig. 1. Result of the external energy balance is the overall heat loss coefficient of the PV-T collector. At the start of iteration process, mean absorber temperature is estimated from input fluid temperature, generally as

$$t_{abs} = t_{in} + 10\,K \qquad (1)$$

External energy balance of the PV-T absorber can be described as

$$\dot{Q}_t + \dot{Q}_e = G \cdot A_a - G \cdot A_a (1 - \tau \cdot \alpha) - \left[U_p \cdot A_G \cdot (t_{abs} - t_a) - U_z \cdot A_G \cdot (t_{abs} - t_a) - U_b \cdot A_b \cdot (t_{abs} - t_a) \right] \qquad (2)$$

where is

A_a aperture area [m^2];

A_G gross area [m^2];

A_b edge area [m^2];

U_p heat loss coefficient for front side of the PV-T collector [W/m^2.K];

U_z heat loss coefficient for back side of the PV-T collector [W/m^2.K];

U_b heat loss coefficient for edge side of the PV-T collector [W/m^2.K].

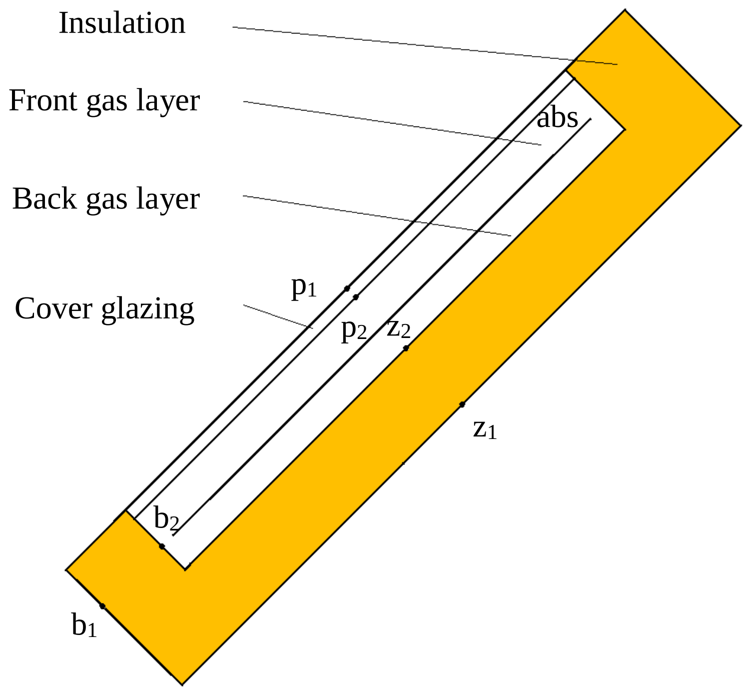

***Fig. 1** Main temperature levels in PV-T collector model*

The heat transfer in PV-T collector can be described by:

- radiation between front side of PV-T absorber and interior surface of cover glazing and radiation between back side of PV-T absorber and interior surface of collector frame;

- natural convection between PV-T absorber and interior surface of cover glazing as well as at interior surface of collector frame;
- heat conduction through cover glazing and heat conduction through thermal insulation of the frame;
- natural and forced convection at exterior surface of cover glazing as well as natural and forced convection at surface collector frame.

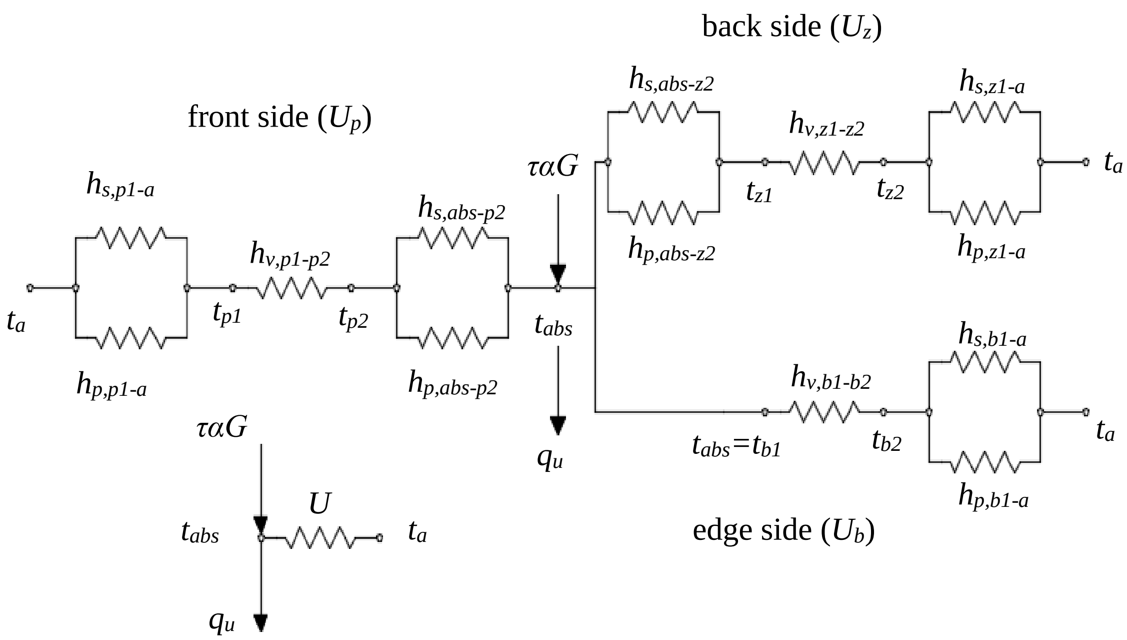

***Fig 2** Schematic detailed layout of external energy balance of PV-T absorber and simplified scheme*

The simplified scheme of external heat transfer balance for the PV-T collector is shown in Fig. 2. Regimes of heat transfer are designated as: v – conduction; p – convection; s – radiation. Initial input parameter for external energy balance is temperature of the PV-T absorber tabs, which is estimated in first step of calculation. In next steps is absorber temperature output of the internal energy balance.

To calculate heat transfer coefficients between main collector surfaces (p1, p2, z1, z2), the surface temperatures are needed but at the start of calculation process the temperatures are not known. In the first iteration step, surface temperatures are estimated from temperature difference between absorber and ambient environment. In this document is specified the basic procedure and correlations which are used in the model.

Heat transfer coefficient for ***radiation between glazing and sky*** is given as

$$h_{s,p1-e} = \varepsilon_{p1} \cdot \sigma \cdot \frac{T_{p1}^4 - T_o^4}{T_{p1} - T_e} \qquad (3)$$

where is

$h_{s,p1-e}$ radiation heat transfer coefficient [W/m^2.K];

T_{p1} temperature of exterior surface of cover glazing [K];

T_o temperature of the sky [K];

T_e ambient temperature [K];

σ Stefan-Boltzmann constant[W/m^2.K^4];

The temperature of the sky was calculated from Swibank correlation [9]

$$T_o = 0,0552 \cdot (T_a)^{1,5}$$

Heat transfer coefficient for ***radiation between absorber and interior surface of cover glazing*** is given as

$$h_{s,abs-p2} = \sigma \cdot \frac{T_{abs}^4 - T_{p2}^4}{\frac{1}{\varepsilon_{p2}} - \frac{1}{\varepsilon_{abs,p}} - 1} \qquad (4)$$

where is

T_{p2} temperature of interior surface of cover glazing [K];

T_{abs} absorber temperature [K];

ε_{p2} emissivity of interior surface of cover glazing [W/m^2.K^4];

ε_{abs} emissivity of front side of absorber [-].

Analogous calculation is for radiation between absorber and interior surface of back frame, as well as for radiation between frame and adjacent ambient surfaces. Radiation between absorber and edge side of the collector is neglected.

Wind convection from glazing to ambient is possible to calculate by large number of relationships and correlations. For solar thermal engineering is commonly used correlation from McAdams [10], as given in equation (3)

$$h_{p,p1-a} = 5,7 + 3,8 \cdot w \qquad (5)$$

where is

$h_{p,p1-e}$ heat transfer coefficient for forced convection [W/m^2.K];

w wind speed [m/s].

Wind convention for back and edge side is determined by eq. (3).

Heat transfer coefficient for ***conduction through glazing*** considering homogeneous insulation structure, thermal conductivity is not function of temperature. Thermal conductance is calculated according to

$$h_{v,p1-p2} = \frac{\lambda_{p1-p2}}{\delta_{p1-p2}} \qquad (6)$$

where is

λ_{p1-p2} thermal conductivity of cover glazing [W/m.K];

δ_{p1-p2} thickness of cover glazing [m].

Analogous calculation is for conduction through insulation of the collector frame.

Natural convection in closed gas layer between absorber and glazing is characterized by Nusselt number. Relationship between heat transfer coefficient and Nusselt number is given as

$$Nu = \frac{h_k \cdot \delta_{abs-p2}}{\lambda_{vzd}} \qquad (7)$$

where is

h_k heat transfer coefficient for natural convection [W/m^2.K];

λ_{vzd} thermal conductivity of the gas in the gas layer[W/m.K];

$\delta_{abs\text{-}p2}$ thickness of gas layer between cover glazing and front surface of absorber [m].

Nusselt number for natural convection is dependent on Rayleigh number, which is product of Grashof number and Prandtl number (Ra=Gr.Pr). Large number of suitable correlations for heat transfer coefficient calculation for the case of natural convection in gas enclosure (closed gas layer) with heat flow upward exists. Correlation according to Matuska [8] was chosen for the model of PV-T collector. Correlation for Nusselt number as function of incidence angle is given as

$$Nu_L = (0{,}1464 - 2{,}602 \cdot 10^{-4} \cdot \beta - 2{,}064 \cdot 10^{-6} \cdot \beta^2) \cdot Ra^{0{,}29} \qquad (8)$$

where is

β slope of the collector [°].

Calculation of ***natural convection between absorber and the back frame*** is different because heat flow direction is downward. Correlation for Nusselt number was chosen from Arnold [11]. Correlation for Nusselt number is given as

$$Nu_L = 1 + \left[Nu_L(\theta = 90°) - 1 \right] \cdot \sin\beta \qquad (9)$$

Overall heat loss coefficient U of the PV-T collector can be calculated as

$$U = U_p + U_z + U_b \frac{A_b}{A_K} \qquad (10)$$

The output of the external energy balance is the overall heat loss coefficient of the PV-T collector $\tilde{U}$ [W/m^{2}K] can be calculated as presented in eq. (12)

$$\tilde{U} = U - r_c \eta_{ref} \tau G \gamma_{ref} \qquad (11)$$

G	incident irradiance [W/m^2];
η_{ref}	reference electrical efficiency [-];
γ_{ref}	temperature coefficient of the PV cell [-];
τ	transmissivity of the glass cover [-];
r_c	packing factor [-].

3.2. Internal energy balance of the PV-T absorber

Based on estimated mean fluid temperature, internal energy flow balance calculations are performed and new value of mean fluid temperature is obtained for next step. Except the usable thermal $\dot{Q}_t$ and electrical output $\dot{Q}_e$ of solar PV-T collector one of the main outputs of internal balance is the absorber temperature t_{abs}. Internal energy absorber balance is processed in simple iteration loop for calculation of correct mean fluid temperature. Schematic energy balance of solar collector with respect to internal absorber energy balance is shown in Fig. 3.

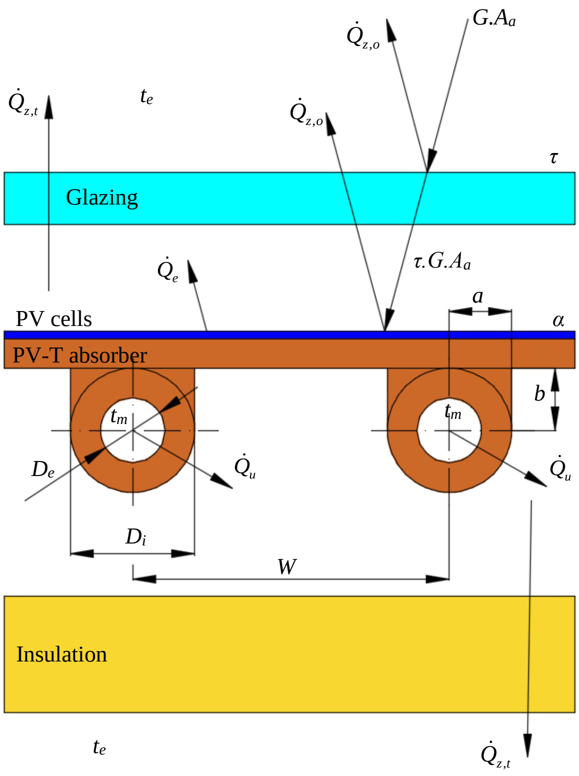

Fig. 3 *Schematic energy balance of PV-T collector with respect to internal absorber energy balance*

Incident irradiance on the cover glazing and absorber is partly reflected. Rest of the irradiance is absorbed by PV-T absorber and converted into the heat and electricity. Part of the heat from the absorber is utilized by heat transfer fluid $\dot{Q}_u$, rest of the heat is dissipated as heat loss $\dot{Q}_{z,t}$ .Part of the incident irradiation is coverted into the electriciy $\dot{Q}_e$.

At the start of iteration process, ***mean fluid temperature t_m*** is estimated from input fluid temperature

$$t_m = t_{in} + 10 \tag{12}$$

Fin efficiency F can be calculated as

$$F = \frac{\tanh\left[m \cdot (W - 2a)/2\right]}{m \cdot (W - 2a)/2} \tag{13}$$

where is

W distance between risers [m];

a average bond width [m].

Parameter m is given as

$$m = \sqrt{\frac{\tilde{U}}{\lambda_{abs} \cdot \delta_{abs}}} \tag{14}$$

where is

λ_{abs} thermal conductivity of the PV-T absorber [W/m.K];

δ_{abs} thickness of the PV-T absorber [m].

Bond thermal conductance for common type of the bond absorber-pipe (Fig. 3) is given as

$$C_{sp} = \frac{\lambda_{sp} \cdot a}{b} \tag{15}$$

where is

λ_{sp} bond thermal conductivity [W/m.K];

b average bond thickness [m].

Forced convection heat transfer coefficient between the fluid and wall of the riser pipe is determined from Nusselt number

$$h_i = Nu\frac{\lambda_f}{D_i} \tag{16}$$

where is

λ_f thermal conductivity of heat transfer fluid [W/m.K];

D_i internal diameter of riser pipes [m].

For laminar forced convection heat transfer in pipes many correlations exist [8]. Shah [12] correlation for laminar forced convection is used in the model. Inverse value of Graetz number can be determine from Reynolds and Prandtl number, which is dimensionless longitudinal coordinate for developing flow. The boundary condition for correlation is dimensionless longitudinal coordinate $x*$, which is defined as

$$x* = Gz^{-1} = \frac{x / D_i}{\mathrm{Re}\cdot \mathrm{Pr}} \tag{17}$$

where is

x riser pipe length [m].

For Shah correlation, the Nusselt number is represented by the following equations

$$Nu_L = \begin{cases} 1.953 \cdot x*^{-1/3} & x* \leq 0.03 \\ 4.364 + \dfrac{0.0722}{x*} & x* > 0.03 \end{cases} \tag{18}$$

In the case of turbulent flow Colburn correlation [13] was used in the form

$$Nu_D = 0.023 \cdot \mathrm{Re}^{4/5} \cdot \mathrm{Pr}^{1/3} \tag{19}$$

The collector ***efficiency factor*** $\tilde{F}'$ defines the thermal quality of a solar absorber. Different absorber configurations result in appropriate equations. For upper bond of absorber to riser pipes the efficiency factor is given as

$$\tilde{F}' = \frac{1/\tilde{U}}{W \cdot \left[\dfrac{1}{\tilde{U}\left[2a + (W-2a)\cdot F\right]} + \dfrac{1}{C_b} + \dfrac{1}{h_i \cdot \pi \cdot D_i} \right]} \qquad (20)$$

where is

W distance between tubes [m];

h_i forced convection heat transfer coefficient in riser pipe [W/m^2.K].

Heat removal factor $\tilde{F}_R$ is defined as the ratio of the actual heat transfer to the maximum heat transfer and may be written as

$$\tilde{F}_R = \frac{\dot{m}\cdot c}{A_a \cdot \tilde{U}} \left[1 - \exp\left(-\frac{A_A \cdot \tilde{U} \cdot \tilde{F}'}{\dot{m}\cdot c} \right) \right] \qquad (21)$$

where is

$\dot{m}$ mass flow rate [kg/s];

c specific heat capacity [J/kg.K];

A_a aperture area [m^2].

The ***photoelectric efficiency*** to determine electrical performance in Florschuetz approach is estimated as a function of ambient temperature t_a, using the relation in the form

$$\eta_a = \eta_{ref}\left[1 - \gamma_{ref}\,(t_a - t_{ref})\right] \qquad (22)$$

where is

t_{ref} reference temperature [°C].

The ***incident energy transformed to heat*** $\tilde{S}$ [W/m^2] can be calculated as

$$\tilde{S} = G \cdot \alpha \cdot \tau \cdot \left(1 - \frac{\eta_a \cdot r_c}{\alpha} \right) \qquad (23)$$

where is

G incident irradiance [W/m^2];

α solar absorptance of the PV-T absorber [-];

τ transmittance of the glass cover [-].

Thermal output $\dot{Q}_t$ [W] is given by

$$\dot{Q}_t = \tilde{F}_R \cdot A_A \left[\tilde{S} - \tilde{U} \cdot (t_{in} - t_a) \right] \tag{24}$$

where t_{in} is the inlet fluid temperature to the collector.

Electrical output $\dot{Q}_e$ [W] is given by

$$\dot{Q}_e = \tau \cdot G \cdot A_A \cdot r_c \cdot \eta_a \cdot \left\{ 1 - \frac{\beta_{ref} \cdot \eta_{ref}}{\eta_a} \cdot \left[\tilde{F}_R (t_{in} - t_a) + \frac{\tilde{S}}{\tilde{U}} \left(1 - \tilde{F}_R \right) \right] \right\} \tag{25}$$

The PV-T ***absorber temperature*** can be calculated as

$$t_{abs} = t_{in} + \frac{\dot{Q}_t / A_a}{\tilde{F}_R \cdot \tilde{U}} \cdot \left(1 - \tilde{F}_R \right) \tag{26}$$

Mean fluid temperature can be calculated as

$$t_m = t_{in} + \frac{\dot{Q}_t / A_a}{\tilde{F}_R \cdot \tilde{U}} \cdot \left(1 - \frac{\tilde{F}_R}{\tilde{F}'} \right) \tag{27}$$

3.3. Optical properties

Incidence angle modifier was simply considered for overall solar radiation G [W/m^2] and the relationship is given as

$$K_\theta = 1 - b_0 \cdot \left(\frac{1}{\cos\theta} - 1 \right) \tag{28}$$

where is

b_0 coefficient of incidence angle modifier [-];

θ incidence angle [°].

4. COMENTS FOR THE CALCULATION

For regime when the mass flow rate is zero, the outlet temperature is calculated as

$$t_{out} = t_a + \frac{\tilde{S}}{\tilde{U}} \tag{29}$$

The type 223 is not yet suitable for analysis of night cooling applications. During the summer night when the temperature in the PV-T collector is lower than ambient temperature, the heat transfer coefficient has to be zero.

5. SPECIAL FEATURES

5.1. Heat transfer fluids models

Mathematical models describing the thermal properties of heat transfer fluids (water, water-etylenglycol mixture, water-propylenglycol mixture) have been taken from [14].

5.2. Front gas layer

In the type 223 is possible to change type of gas in the front gas layer between glazing and PV-T absorber from air to argon (parameter number 38).

5.2.1. Dry air

Dynamic viscosity [Pa.s]

For temperature range from -20 to 200 °C

$$10^6 \eta = \frac{1,49 \cdot T^{1,5}}{T + 117} \tag{30}$$

Density [kg/m^3];

$$\rho = \frac{p}{287 \cdot T} \tag{31}$$

Specific thermal capacity [J/kg.K]

For temperature range from -20 to 500 °C

$$c = 1010 + 0,12 \cdot t \tag{32}$$

Thermal conductivity [W/m.K]

For temperature range from -20 to 200 °C

$$\lambda \cdot 10^3 = \frac{2,27 \cdot T^{1,5}}{T + 160} \tag{33}$$

5.2.2. Argon

Correlations are for temperature range from 0 to 150 °C, for 100 % concentration of Argon.

Dynamic viscosity [Pa.s]

$$\eta = 6 \cdot 10^{-8} \cdot T + 5 \cdot 10^{-6} \tag{34}$$

Density [kg/m^3]

$$\rho = -0,0042 \cdot T + 2,873 \tag{35}$$

Specific thermal capacity [J/kg.K]

$$c = 3 \cdot 10^{-5} \cdot T^2 - 0,0301 \cdot T + 527,44 \tag{36}$$

Thermal conductivity [W/m.K]

$$\lambda = 5 \cdot 10^{-5} \cdot T + 0,0035 \tag{37}$$

6. LICENSE, SOURCE CODE AND INSTALLATION

The Type223 component can be ordered at e-mail address tomas.matuska@fs.cvut.cz

6.1. Installation

The Type223 collector model is a TRNSYS17 drop-in dll component. For a complete set of files one should have:

Type223.dll – the drop-in dll file

Type223.cpp – the C++ source code

Type223.tmf – the Simulation Studio proforma

Type223.bmp – the Simulation Studio proforma icon

For installation:

1. Copy the .dll file to \TRNSYS17\UserLib\ReleaseDLLs\

2. Copy the .tmf and .bmp files to the \Proformas folder, e.g. C:\Trnsys17\Studio\Proformas\Nonstandard\

3. Restart simulation studio if it was running.

7. OUTLOOK FOR FUTURE DEVELOPMENT

Following work will be to extend the model by the dynamic part. Also the model will be extend by incidence angle modifier for diffuse radiation and reflected radiation.

ACKNOWLEDGEMENT

Development of energy active curtain walling has been financially supported by Technology Agency of Czech Republic in the frame of research project TA04021195.

LITERATURE

[1] TRNSYS Manual, 2006. TRNSYS 16 a TRaNsient SYstem Simulation program. In: Mathematical Reference, vol. 5. Solar Energy Laboratory, University of Winconsin–Madison.

[2] Duffie, J.A., Beckman, W.A., 1991. Solar Engineering of Thermal Processes, 2nd ed. Wiley, New York.

[3] Bergene, T., Lovvik, O., 1995. Model calculations on a flat-plate solar heat collector with integrated solar cells. Sol. Energy 55, 453–462.

[4] Zondag, H.A., De Vries, D.D., Van Helden, W.G.J., Van Zolingen, R.J.C., Van Steenhoven, A.A., 2002. The thermal and electrical yield of a PV–thermal collector. Solar Energy 72, 113–128.

[5] Chow, T.T., 2003. Performance analysis of photovoltaic–thermal collector by explicit dynamic model. Solar Energy, vol. 75, 143–152.

[6] Haurant, P., Ménézo, CH., Gailard, L. Dupeyrat, P., 2015. Dynamic numerical model of a high efficiency PV-T collector integrated into a domestic hot water system, Solar Energy 111, 68-81.

[7] Florschuetz, W. L. 1979. Extension of the Hottel-Whilier model to the analysis of combined photovoltaic/thermal flat plate collector. Solar Energy, vol. 22, pp. 361-366.

[8] Matuska, T., Zmrhal V., KOLEKTOR 2.2 - Computer Program for Efficiency Calculation of Solar Flat-Plate Collectors. 2009.

[9] Swinbank, W., C.: Long-wave radiation from clear skies. Quarterly Journal of Royal Meteorological Society 89, pp. 339-348, 1963.

[10] McAdams,W. H. Heat Transmission, 3rd edition. McGraw-Hill, New York. pp. 249. 1954.

[11] Arnold, Catton, Edwards: Experimental investigation of natural convection in inclined rectangular regions of differing aspect ratios. ASME Paper 75-HT-62, 1975.

[12] Shah, R. K., London, A. L.: Laminar flow forced convection in ducts. 1st edition. New York: Academic Press. 1978.

[13] Colburn, A. P.: Trans. AIChE, 29, 174, 1933.

[14] Conde, M.: Thermophysical properties of brines – Models, Conde Engineering, http://www.mrc-eng.com, Zurich 2002.